

Strength and behaviour of reinforced SCC wall panels in one-way action

*N. Ganesan, P.V. Indira^a and S. Rajendra Prasad^b

Department of Civil Engineering, National Institute of Technology Calicut, Kerala State,
673601, India

(Received June 13, 2009, Accepted March 24, 2010)

Abstract. A total of 28 wall panels were cast and tested under uniformly distributed axial load in one-way in-plane action to study the effect of slenderness ratio (SR) and aspect ratio (AR) on the ultimate load. Two concrete formulations, normal concrete (NC) and self compacting concrete (SCC), were used for the casting of wall panels. Out of 28 wall panels, 12 were made of NC and the remaining 16 panels were of SCC. All the 12 NC panels and 12 out of 16 SCC panels were used to study the influence of SR and the remaining 4 SCC panels were tested to study the effect of AR on the ultimate load. A brief review of studies available in literature on the strength and behaviour of reinforced concrete (RC) wall panels is presented. Load-deformation response was recorded and analyzed. The ultimate load of SCC wall panels decreases non-linearly with the increase in SR and decreases linearly with increasing values of AR. Based on this study a method is proposed to predict the ultimate load of reinforced SCC wall panels. The modified method includes the effect of SR, AR and concrete strength.

Keywords: self-compacting concrete; bearing walls; slenderness ratio; aspect ratio; one-way action; crushing; buckling.

1. Introduction

Reinforced concrete (RC) wall panels are used as load bearing structural elements in buildings. Generally, the loads acting on the wall panels are in-plane axial loads, but often they become eccentric due to constructional imperfections. The thickness of the wall, when compared to other dimensions, is small and introduces the slenderness effect leading to problems of stability. Slenderness ratio (SR) is defined as the ratio of height to thickness (h/t) of wall panel. Also depending on the relative ratio of height to length (h/L), called aspect ratio (AR), the behaviour of wall panel under load would vary from a wide short compression member to a narrow deep slender member. Development of satisfactory design procedure for the wall panel, therefore, requires a good understanding of its strength and behaviour which is influenced by its geometry, support conditions and materials of construction.

*Corresponding author, Professor, E-mail: ganesan@nitc.ac.in

^aProfessor, E-mail: indira@nitc.ac.in

^bResearch Scholar, E-mail: rajendra_sunke@yahoo.co.in

Several attempts have been made in the past to study the strength and behaviour of RC walls under one-way and two-way actions. Based on such investigations design equations have been proposed to predict the load carrying capacity of RC walls. The equations to predict the ultimate load, obtained from these methods, have been incorporated in the international codes of practice for estimating the ultimate load of wall panels (Oberlender and Everard 1977, Kripanarayanan 1977). Major concrete codes now consider RC walls as important structural elements and have devoted separate sections to wall design. Also attempts have been made to compare some of the equations available in literature with the experimental values reported by other researchers (Doh 2002).

Recently self compacting concrete (SCC) has gained much attention in the concrete industry and is used in many applications successfully throughout the world (Domone 2006). The workability of SCC is higher than the highest class of workability associated with normal high performance concrete, typically used in pre-cast concrete fabrication. This increased flowability of SCC can ease the constructability requirements of precast elements whose important aspect of the design is the ability to place and consolidate concrete within the form and around the internal reinforcing (PCI guide lines 2003).

Though the SCC load bearing wall panels produced by precast concrete industry are being increasingly used in building systems, investigations on their strength and behaviour are not yet reported. Hence a large scale experimental investigation was recently carried out at the National Institute of Technology, India. This paper is a part of this experimental investigation along with the development of a method to predict the ultimate load of SCC wall panels.

2. Review of earlier studies

Summary of review of literature is presented in Table 1 and the equations proposed by various researchers to predict the ultimate load of wall panels in one-way action are given in Table 2. The review of earlier work along with the comparison of equations available in the literature was published in detail elsewhere (Ganesan *et al.* 2009).

3. Experimental investigation

The experimental programme consisted of casting and testing of 28 wall panels under compression. Two concrete formulations, normal concrete (NC) and self compacting concrete (SCC), were used for the casting of wall panels. Out of these 28 wall panels, 12 were made using NC and the remaining 16 were made of SCC. All the 12 NC panels (3 specimen for each value of SR) and 12 out of 16 SCC panels (3 specimen for each value of SR) were used to study the influence of SR and the remaining 4 SCC panels were tested to study the effect of AR on the ultimate load of wall panels. Table 3 gives the details of over all dimensions, SR and AR of wall panels.

3.1 Materials used

The materials consisted of Portland Pozzolana Cement (PPC-Fly ash based) conforming to IS 1489 (Part 1) (1991), fine aggregate conforming to grading zone III of IS 383 (1970) having a

Table 1 Salient details of one-way action tests on normal concrete and high strength concrete panels available in literature

Investigator	Year	No. of tests	Strength of Concrete, f'_c (N/mm ²)	Slenderness ratio (h/t)	Aspect ratio (h/L)	Percentage of Steel		Eccentricity	Findings	
						Single layer	Double Layer		Small value of SR	Large value of SR
Oberlender and Everard	1977	54	28.00 to 42	8 to 28	1 to 3.50	0.33	0.47	$t/6$	Failed by crushing	Failed by buckling
Pillai and Parthasarathy	1977	18	16.00 to 31.50	5 to 30	0.57 to 3.00	0.15 and 0.30	*	$t/6$	Influence of steel ratio on the ultimate load was found to be negligible	
Kripanarayanan	1977	Theoretical	28.00	0 to 32	0 to 0.66	*	*	$t/6$	When the percentage of reinforcement was in between 0.75% and 1.0% of cross sectional area of wall, the load carrying capacity was found to increase considerably	
Saheb and Desayi	1989	24	16.14 to 20.14	9 to 27	0.67 to 2.00	*	0.17 to 0.86	$t/6$	Failure by crushing near edges	Buckling failure was predominant
Fragomeni	1995	20	32.90 to 67.40	12 to 25	2 to 5	0.25 to 0.31	*	$t/6$	The position of reinforcement did not affect the failure mode	
J. H. Doh	2002	6	35.70 to 75.90	30 to 40	1	0.31	*	$t/6$	The value of axial strength ratio decrease gradually with increasing values of SR	
Benayoune <i>et al.</i>	2007	6	25.40	10.77 to 20	1.22 to 2.00	NA	NA	Axial loading	The strength of panels decreased non-linearly with the increase of the slenderness ratio.	
ACI 318-2008	2008			≤ 25		0.15% and 0.25% in the vertical and horizontal directions		$\leq t/6$		
N. Ganesan <i>et al.</i>	2009	8	34.14	12 to 30	0.75 to 1.875	0.88% and 0.74% in the vertical and horizontal directions.		$t/6$	International equations have been compared and noted that the equation of Pillai and Parthasarathy was found to give better comparison with the experimental results.	

Note 1. * Not considered in their experiments
 2. NA Not Available in the literature

Table 2 Formulae proposed by various researchers to predict ultimate load of walls in one-way action

Researcher	Proposed equation to predict the ultimate load
Oberlender & Everard (1977)	$P_u = 0.6\phi f'_c L t [1 - (h/30t)^2]$
Pillai & Parthasarathy (1977)	$P_u = 0.57\phi f'_c L t [1 - (h/50t)^2]$
Kripanarayanan (1977)	$P_u = 0.55\phi f'_c L t [1 - (kh/32t)^2]$
Saheb & Desayi (1989)	$P_u = 0.55\phi [A_g f'_c + (f_y - f'_c) A_{sv}] \{1 - (h/32t)^2\} \{1.2 - (h/10L)\}$, for $h/L < 2.0$ $P_u = 0.55\phi [A_g f'_c + (f_y - f'_c) A_{sv}] \{1 - (h/32t)^2\}$, for $h/L \geq 2.0$
Fragomeni (1995)	$\phi N_u = \phi (t - 1.2e - 2e_a) 0.6 f'_c$, when $20 \leq f'_c \leq 50$ $\phi N_u = \phi (t - 1.2e - 2e_a) 30 [1 + (f'_c - 50)/80]$, when $50 \leq f'_c \leq 80$
Doh (2002)	$\phi N_u = \phi 2.0 f'_c {}^{0.7} (t - 1.2e - 2e_a)$
Benayoune <i>et al.</i> (2007)	$P_u = 0.4 f_{cu} A_g [1 - (kh/40t)^2] + 0.67 f_y A_{sc}$
ACI 318-2008	$\phi P_n = 0.55\phi f'_c L t [1 - (kh/32t)^2]$

Table 3 Details of wall panels and variables

Type	Panel Designation	Specimens Tested (Nos.)	Panel Size (h×L×t)(mm)	Variables	
				SR	AR
NC	OWSRN-1	3	480×320×40	12	1.5
	OWSRN-2	3	600×400×40	15	
	OWSRN-3	3	840×560×40	21	
	OWSRN-4	3	1200×800×40	30	
SCC	OWSRS-1	3	480×320×40	12	1.5
	OWSRS-2	3	600×400×40	15	
	OWSRS-3	3	840×560×40	21	
	OWSRS-4	3	1200×800×40	30	
SCC	OWARS-1	1	600×320×40	15	1.875
	OWARS-2	1	600×400×40		1.5
	OWARS-3	1	600×560×40		1.07
	OWARS-4	1	600×800×40		0.75

Table 4 Properties of portland pozzolana cement

Sl. No.	Properties	Values
1.	Specific gravity	2.94
2.	Normal consistency	31%
3.	Initial setting time	170 minutes
4.	Final setting time	350 minutes
5.	Compressive strength	
	3 days	20.4 MPa
	7 days	30.0 MPa
	28 days	52.0 MPa

Table 5 Properties of silica fume

Sl. No.	Particulars	Properties
1	Specific gravity	2.2
2	SiO ₂	90.3%
3	Moisture content	0.60%
4	Loss on ignition at 975°C	2.10%
5	Carbon	0.80%
6	>45 Microns	0.40%
7	Bulk density	640 g/cc

Table 6 Details of fly ash - class C

Sl. No.	Properties/Constituents	Observed value	Requirements as per IS: 3812-2003
1	Fineness (cm/gm)	3809	> 3200
2	Lime reactivity (MPa)	6.24 MPa	4.0 MPa
3	Soundness (Lechatlier) (mm)	2 mm	< 10
4	Specific gravity	2.55	-
5	SiO ₂ +Al ₂ O ₃ +Fe ₂ O ₃ (% wt)	95.88	> 70
6	SiO ₂ (% wt)	47.50	> 35
7	MgO (% wt)	2.38	< 5
8	SO ₃ (% wt)	1.66	< 2.75
9	Na ₂ O (% wt)	0.57	< 1.5
10	CaO (% wt)	8.71	-
11	Loss on ignition (% wt)	2.23	< 12.0

specific gravity of 2.67, coarse aggregate having a maximum size of 12.5 mm with specific gravity of 2.78 and potable water. The properties of cement are presented in Table 4. Mineral admixtures which consisted of silica fume and class-C fly ash and chemical admixtures comprised of naphthalene based super plasticizer and polysaccharide based viscosity modifying agent (VMA) were used. The details of silica fume and fly ash are given in Tables 5 and 6 respectively.

3.1.1 Reinforcement

The reinforcement in the form of rectangular grid, fabricated using 6 mm diameter High Yield Strength Deformed bars (Fe 415), was placed in a single layer at mid thickness of the panels. The spacing of bars (100 mm) in both directions did not exceed three times the panel thickness, which is a maximum thickness as per ACI 318 (2008), with a clear side cover of 10 mm. The yield strength of reinforcing steel was 445 N/mm². The percentages of vertical and horizontal reinforcement provided in the panels are 0.88 and 0.74 respectively. Typical arrangement of reinforcement is shown in Fig. 1.

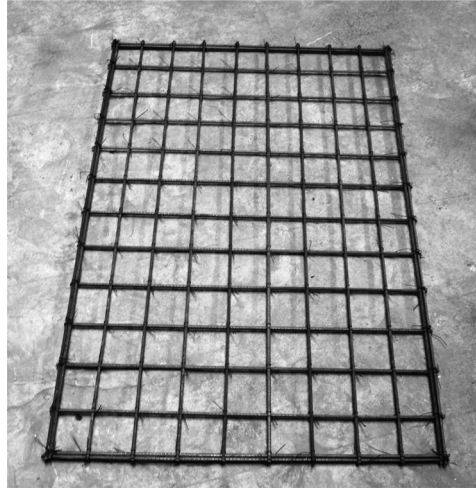


Fig. 1 Typical arrangement of reinforcement

3.2 Development of SCC

The normal concrete (NC) was designed for a characteristic compressive strength of M30 grade as per IS 10262 (1982) and the mix proportions thus obtained are presented in Table 7. The mix proportions of SCC were obtained after extensive trials based on the guidelines of EFNARC (2002) for M30 grade concrete. As per EFNARC (2002), the concrete can be considered as self compactable if it fulfills the requirements of filling ability, passing ability and segregation resistance. In the process of development, the properties of fresh concrete formulated with trial mixes were tested to verify the self compactability. The mix proportions of concrete which satisfied the requirements of EFNARC (2002) for self compactability are considered for the mix of SCC used in the present study. While checking the properties of this mix in fresh state for self compactability, it was noted that the time required, to empty the V-funnel, was 8 seconds. The slump flow by Abrams cone was found to be 650 mm. The ratio of h_2/h_1 of L-box test was found to be 0.9. For checking the segregation resistance, V-funnel at $T_{5\text{minutes}}$ test was conducted. The trap door of the V-funnel was opened 5 minutes after filling and it was observed that the time required to empty the V-funnel was found to be 11 seconds. The properties of SCC in fresh state are presented in Table 8 and the constituents of SCC mix thus obtained are presented in Table 9.

Table 7 Mix proportions of normal concrete

Particulars	Quantity (kg/m ³)
Cement	380
Fine aggregate	615
Coarse aggregate	1185
Water	171

Table 8 Properties of SCC in fresh state

Sl. No	Test method	Unit	Requirement as per EFNARC	Observed value in the experiment
1	Slump flow	mm	650 - 800	650
2	T _{50cm} slump flow	Sec	2 - 5	4
3	V-funnel	Sec	6 - 12	8
4	Time increase, V-funnel at T _{5minutes}	Sec	0 - (+3)	11
5	L-box	(h ₂ /h ₁)	0.8 - 1.0	0.9

Table 9 Mix proportions of SCC

Particulars	Quantity (kg/m ³)
Cement (Fly ash based)	493
Fly ash	20
Silica fume	10
Fine aggregate	789
Coarse aggregate	740
Water	246
Superplasticiser	5
VMA	0.012

3.3 Casting of specimens

For casting the specimens, the formwork was fabricated using Indian Standard (IS) equal angles of 40 mm × 40 mm × 6 mm. The specimens were cast horizontally on a level floor in the Structural Engineering Laboratory. The thickness of the wall panels was kept constant through out. After casting, the wall panels were covered with moist hessian and polyethylene plastic sheets to prevent moisture loss. The formwork was removed 24 hours after casting and the specimens were covered with moist hessian for an initial period of three days and then immersed in the curing tank on the fourth day. After 28 days of curing, the panels were taken out from the curing tank and white washed and made ready for testing. Three 150 mm size control cubes were cast along with the wall panels for each series and tested on the day of testing of panels.

3.4 Testing of wall panels

All specimens were subjected to loading in the vertical position in a Compression Testing Machine of 2,940 kN (300 tons) capacity. A leveling ruler was used to ensure the proper leveling of the panels. Plumb-bob was used to ensure verticality of the panels. Pinned end condition was simulated at both the supporting ends and uniformly distributed load was applied at a small eccentricity of $t/6$ to reflect possible eccentric load in practice, as carried out by other investigators (Oberlender and Everard 1977, Saheb and Desayi 1989, Doh 2002). The rate of loading was 24.5 kN (2.5 tons) per minute. Fig. 2 shows the details of test set up and Figs. 3(a) and 3(b) show the schematic diagram of test set-up and details at bottom hinged edge respectively. The loading

was gradually increased in stages up to failure. At each stage, lateral deformations at quarter and mid height points along the central vertical line of the panel were measured using LVDTs. The experimental ultimate loads (P_{ue}) were recorded and presented in Table 10.

As the SR and over all dimensions are varying for the panels, the values of ultimate loads were

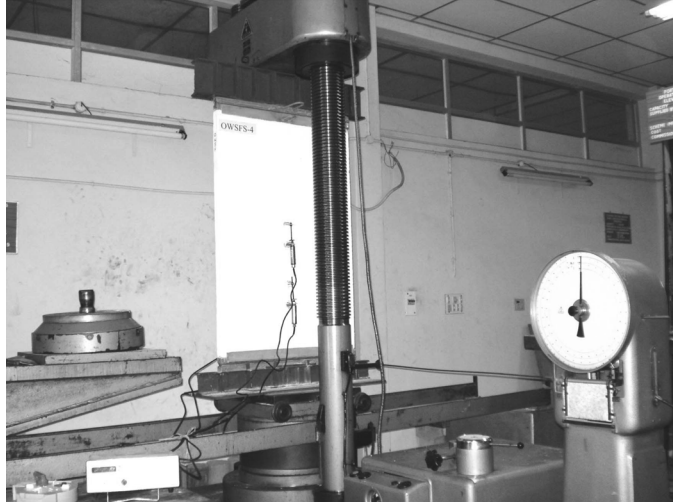
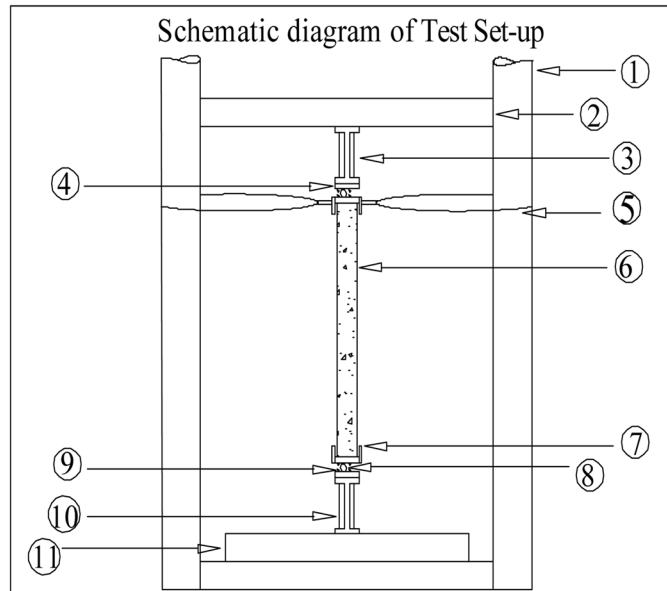


Fig. 2 Test set-up



- (1) Column of the testing machine (2) Cross head of the testing machine (3) Stiffened steel girder (top support for panel) (4) 40 mm×24 mm bearing plate (5) Chain (6) Specimen (7) Guide plate (8) 16 mm diameter roller (9) 4 numbers of 6 mm diameter guide bars for roller (10) stiffened steel girder (bottom support for panel) (11) Lower compression plate

Fig. 3(a) Schematic diagram of test set-up

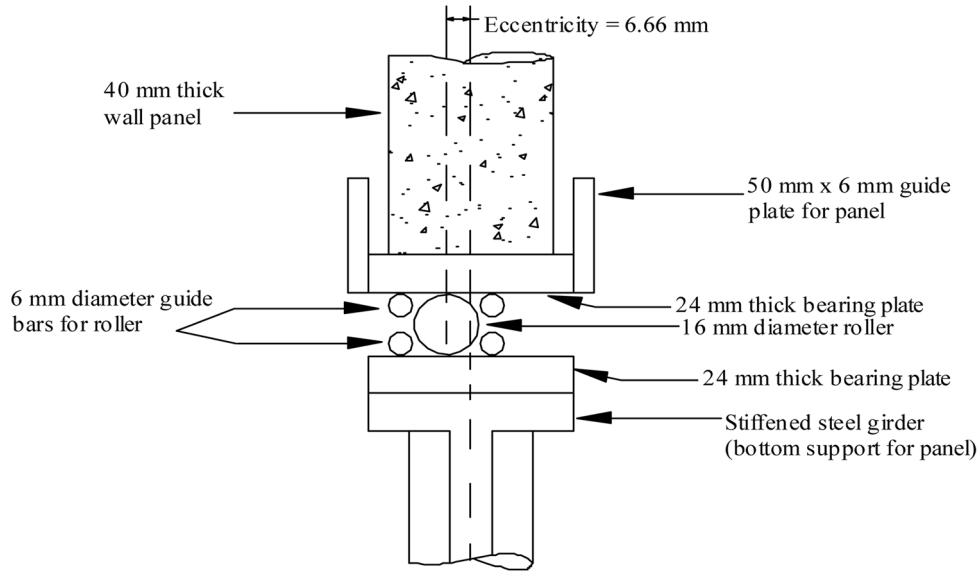


Fig. 3(b) Details at bottom hinged edge

Table 10 Experimental ultimate loads

Panel designation	f_{cu} (N/mm ²)	Experimental ultimate load (P_{ue}) (kN)	Experimental axial strength ratio $P_{ue}/f_c'Lt$	Axial strength ratios ($P_u/f_c'Lt$) using the equations of			
				Oberlender	Pillai and Parthasarathy	Saheb and Desayi	ACI 318 - 2008
OWSRN-1	42.67	294.00	0.67	0.50	0.54	0.56	0.47
OWSRN-2		333.20	0.61	0.45	0.52	0.51	0.43
OWSRN-3		450.80	0.59	0.31	0.47	0.37	0.31
OWSRN-4		362.60	0.33	*	0.36	0.08	0.066
OWSRS-1	43.56	303.80	0.68	0.50	0.54	0.56	0.47
OWSRS-2		352.80	0.63	0.45	0.52	0.51	0.43
OWSRS-3		480.20	0.62	0.31	0.47	0.37	0.31
OWSRS-4		465.50	0.42	*	0.36	0.08	0.066
OWARS-1	43.56	240.10	0.54	0.45	0.52	0.49	0.43
OWARS-2		352.80	0.63	0.45	0.52	0.51	0.43
OWARS-3		499.80	0.64	0.45	0.52	0.53	0.43
OWARS-4		705.60	0.63	0.45	0.52	0.55	0.43

Note: 1. While computing the values of ultimate load (P_u) using ACI 318-2008 and other equations, ϕ is taken as unity. This will represent the actual values of ultimate load with out any reduction factor.

2. * indicates that the equation of Oberlender and Everard yields zero ultimate load for the walls with SR = 30.

normalized by dividing experimental ultimate load (P_{ue}) by the parameter ($f'_c Lt$). These normalized values, called as experimental axial strength ratios of panels $\{P_{ue}/(f'_c Lt)\}$, are also presented in Table 10. Referring to the table, it may be noted that the experimental axial strength ratios decrease with increase of SR in the case of both NC and SCC wall panels. Comparison of NC and SCC wall panels for the same SR shows a marginal increase in the values of ultimate load in all these specimens.

Three 150 mm size control cubes which were cast along with the wall panels for each series were tested on the day of testing of panels. The values of cube compressive strength of concrete (f_{cu}) of different series are given in Table 10. From the Table it is evident that the increase in 28 days compressive strength of SCC, though the fines (cement, fly ash and silica fume) content was more in SCC mix, than NC is marginal. This may be attributed to the reduced content of coarse aggregate, increase in w/c (0.45 to 0.50) ratio and the addition of superplasticiser in SCC mix to achieve the flowability.

4. Discussion of test results

4.1 Crack patterns and failure mode

The crack patterns observed on both the tension and the compression faces of the panels indicated the following; (i) the NC specimens OWSRN-1 and OWSRN-2 failed by crushing near the bottom edges, (ii) panel OWSRN-3 failed by bending type of failure at mid height by forming central horizontal cracks on tension side and crushing on compression side, and (iii) OWSRN-4 failed by bending at mid height by developing more central horizontal cracks than OWSRN-3. In general, in the case of wall panels having SR less than 21, it was found that normal concrete walls tended to crush before the yielding of the reinforcement. The failure pattern of SCC wall panels is similar to those of NC panels for the SR up to 15. Unlike OWSRN-3, OWSRS-3 failed by crushing near the edges. However the failure pattern of OWSRS-4 is different from the wall panels having SR less

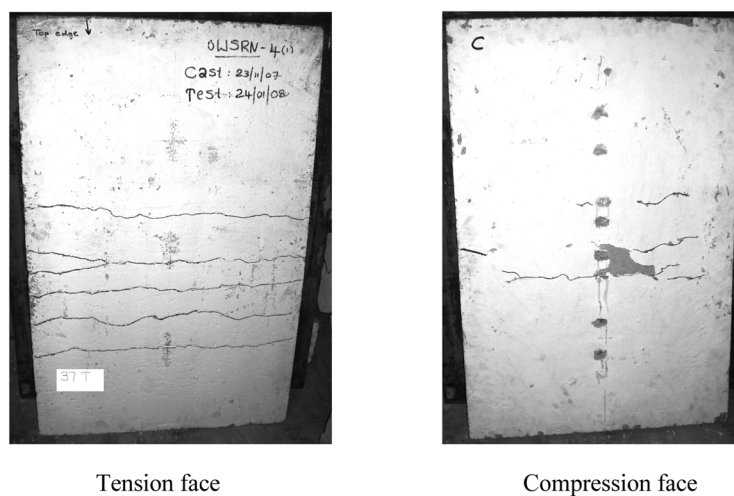


Fig. 4 Crack pattern of NC (OWSRN-4) specimen

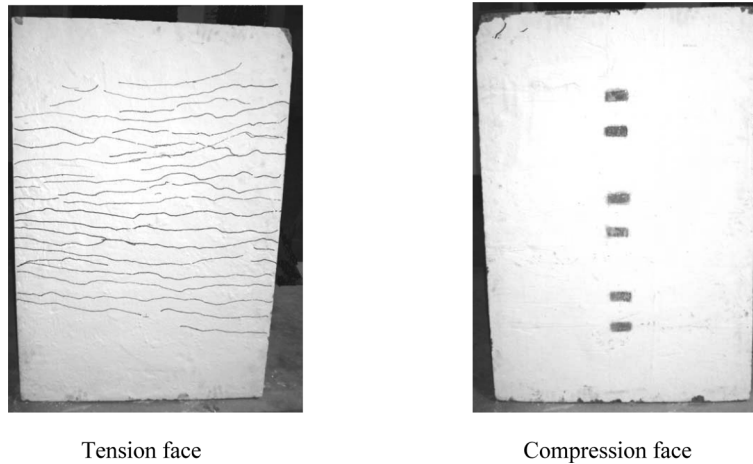


Fig. 5 Crack pattern of SCC (OWSRS-4) specimen

than 21. Large number of finer cracks developed in the case of SCC wall panels with values of SR higher than 21. This may be attributed to the high volume of finer particles in SCC mix than that of NC mix. This produces preliminary microcracking when the SCC wall panels are subjected to high compressive stresses as noted by other researchers (Luciano and Andrea 2008). Another important observation noted was that the shape of the SCC panel after failure and until removed from the testing machine was in single curvature form. When the loading was completely removed the panel started straightening and it has regained about 75% of its preloaded linear shape. This indicates that SCC wall panels are more ductile than NC panels. All panels deflected in a single curvature in the vertical direction with maximum deflection occurring along the centre of the panels. All SCC panels of OWARS series, except the panel with $AR = 1.875$, failed by crushing near the edges. The panel with $AR = 1.875$ failed by crushing accompanied by significant lateral deflections. Fig. 4 shows typical crack patterns of NC specimens and Fig. 5 shows typical crack patterns of SCC specimens for the value of $SR = 30$.

4.2 Load - Deformation response

The load versus lateral deflection curves of wall panels are shown in Figs. 6-12. The maximum deflections were noted just prior to the ultimate load. The sudden failure of the panels made it difficult to record deflection precisely at failure. Thus, in the load-deflection plots, the absolute maximum ultimate loads and the corresponding maximum deflections are not shown. Fig. 6 shows the load versus lateral deflection plots of NC wall panels for varying values of SR. It may be noted from the figure that the curves are linear up to the formation of the first crack and beyond which they exhibit non-linearity. In general, as SR increases the load carrying capacity decreases and the lateral deflection increases for all the specimens. However a significant increase of lateral deflection can be seen in the case of wall panels for $SR = 30$. The continuously increasing values of deflection as the loading increases indicate that the wall panels exhibit a smooth ductile type of failure till the ultimate load is reached. Similar observations were noted in the case of SCC wall panels. The load versus lateral deflection plots of SCC wall panels for different values of SR are given in Fig. 7. In this case also initially the curves are linear up to the formation of first crack, beyond which they

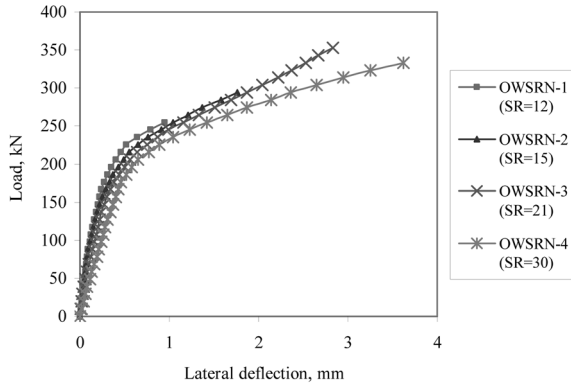


Fig. 6 Effect of slenderness ratio in NC wall panels

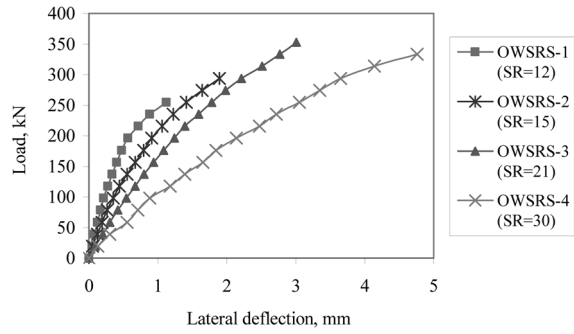


Fig. 7 Effect of slenderness ratio in SCC wall panels

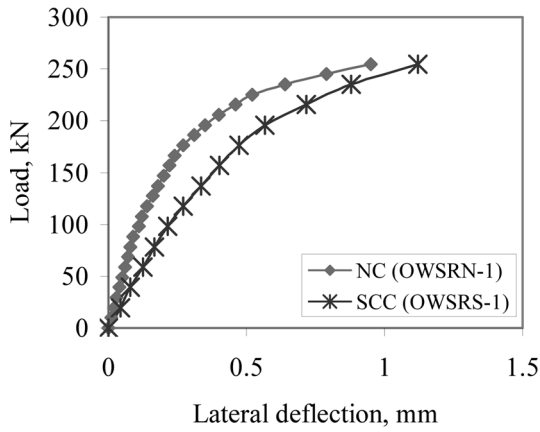


Fig. 8 Comparison of NC and SCC wall panels for SR = 12

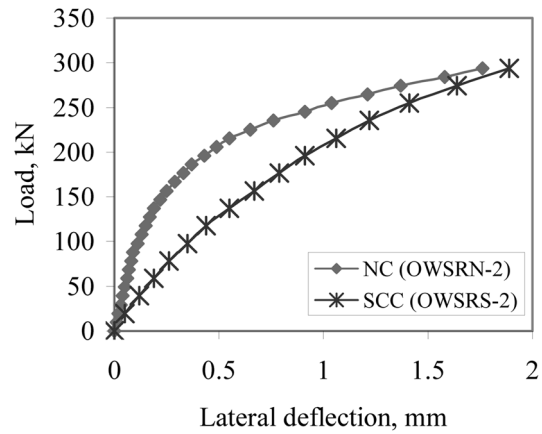


Fig. 9 Comparison of NC and SCC wall panels for SR = 15

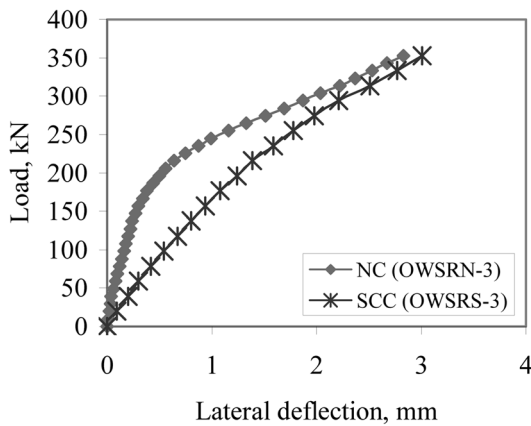


Fig. 10 Comparison of NC and SCC wall panels for SR = 21

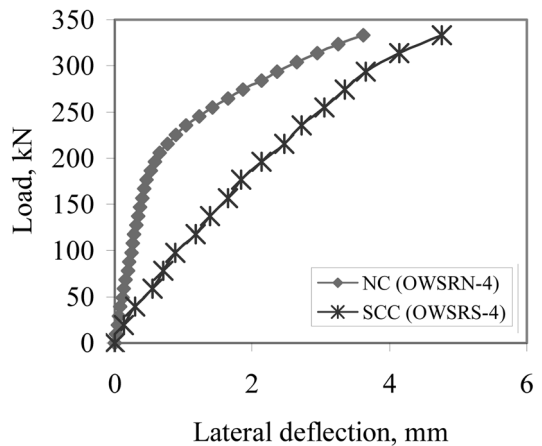


Fig. 11 Comparison of NC and SCC wall panels for SR = 30

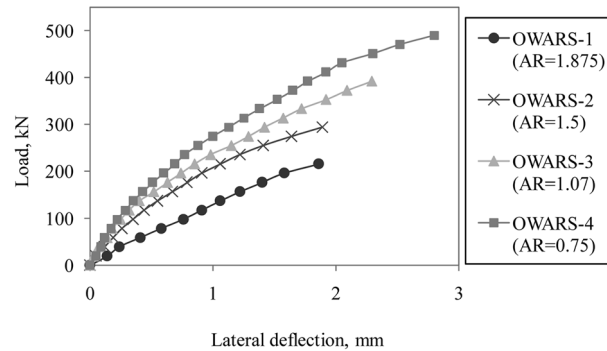


Fig. 12 Effect of aspect ratio in SCC wall panels

exhibit non-linear characteristics. However comparing the load-deflection plots of NC and SCC wall panels (Figs. 8 to 11), it may be noted that the initial slope of the load-deflection curve is steeper in the case of NC panels than those of SCC panels. This indicates that SCC wall panels exhibit softening behaviour which means that the SCC wall panels behave in a more ductile manner than the NC wall panels. As mentioned earlier this type of softening of material is due to the presence of higher percentage of finer particles in the case of SCC panels which transforms the material to behave in a ductile manner and also induces higher degree of compressibility.

The load versus lateral deflection curves of OWARS series are shown in Fig. 12. From the figure it may be noted that the wall panel with AR = 1.875 has suffered maximum deflection than those panels with low values of AR. This may be due to the behaviour of wall panel as, (i) narrow deep slender member when the AR = 1.875 and (ii) wide short compression member when the AR = 0.75. The effect of AR on the ultimate load is further discussed in the subsequent section.

4.3 Influence of parameters on ultimate load

To study the influence of SR and AR on the strength and behaviour of SCC wall panels, separate plots have been drawn between (P_{ue}/P_{us}) and SR or AR, where P_{ue} represents the experimental ultimate load and P_{us} represents theoretical ultimate load which is obtained using the material properties. These plots are shown in Figs. 13 and 14 respectively. From the Fig. 13, it may be noted that the strength of wall panel decreases non-linearly with increase in SR. The reduction in strength is about 38.23% for increase of SR from 12 to 30. From the Fig. 14, it may be noted that the strength of wall panel decreases linearly with the increase of AR. The reduction in strength is about 14.29% for an increase of AR from 0.75 to 1.875. From an observation of the failure of specimens, it may be noted that the failure occurred predominantly by crushing in the panel with AR = 0.75 (Fig. 8), while in the case of panels with higher values of AR, the failure occurred by bending (Figs. 5 to 7). Significantly, the wall panel with AR = 1.875 failed by developing fine cracks in the mid height and exhibiting reduction in ultimate load. This may be attributed to the following reasons. The wall panel with low value of AR will behave like a wide short compression member. In this case, the member may be assumed to have hypothetical strips called middle and end strips as shown in Fig. 15. Even though a uniformly distributed load is applied on this wide short compression member, the resistance offered by the end strips will be relatively less than the middle strip because of the free edge conditions of the end strips. This difference in the resistance would

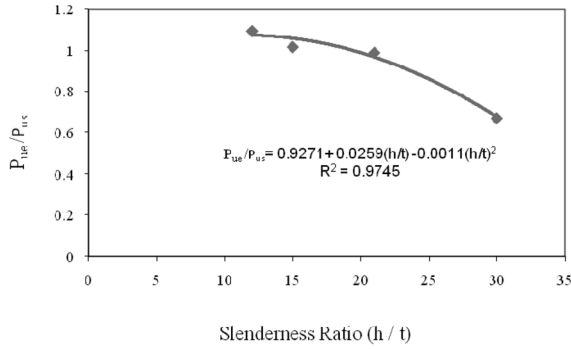


Fig. 13 Influence of SR on ultimate load

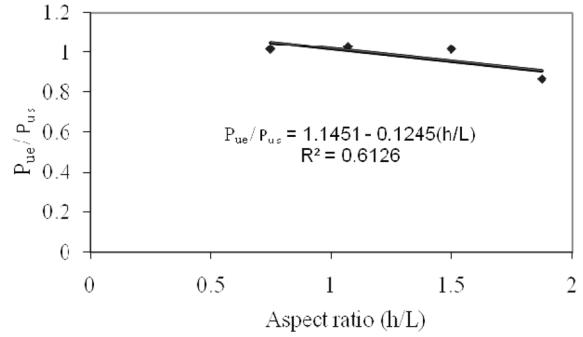


Fig. 14 Influence of AR on ultimate load

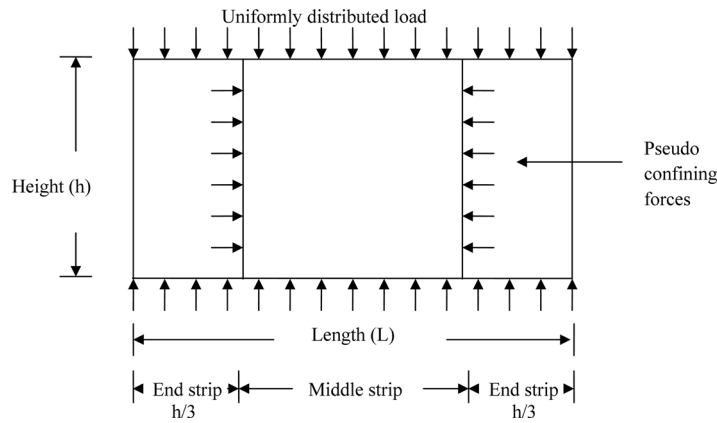


Fig. 15 Hypothesis for the influence of AR on ultimate load of wall panel

result in the development of pseudo confining forces which act on the middle strip and improve the load carrying capacity. From the observation of failure, it may be assumed that the width of end strip could be about one third of the height of the panel. On the other hand, wall panel with higher value of AR will behave like a narrow deep slender member. In such member there is no possibility of the development of confining forces from the end strips because the entire member will act as single member without the feasibility of having end strips.

5. Comparison of international equations with experimental results

An attempt is made to compare the equations, available in literature for predicting the ultimate load of RC wall panels, with the experimental results of this study. For this comparison, the equations of Oberlender and Everard (1977), Pillai and Parthasarathy (1977), Saheb and Desayi (1989) and ACI 318 (2008) were used. The values of ultimate load (P_u) were computed using these equations and normalised by dividing them (P_u) by the parameter ($f'_c Lt$). These values of axial strength ratios are given in Table 9. This Table is reproduced in Fig. 16 for more clarification and quick reference.

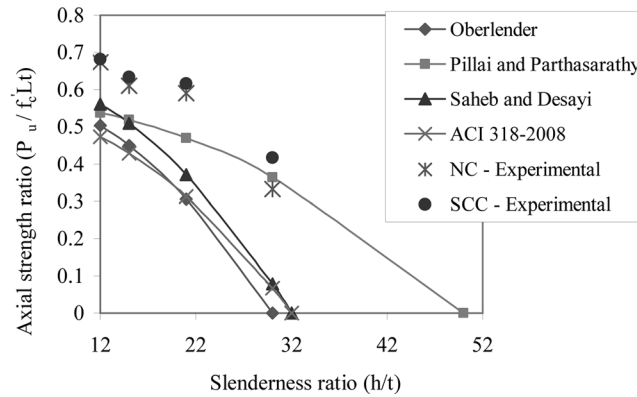


Fig. 16 Comparison of different equations and experimental values

From the Fig. 16 it may be noted that the values of axial strength ratios predicted by the equations of Oberlender and Everard (1977), Saheb and Desayi (1989) and ACI 318 (2008) were highly conservative. On the other hand the values of axial strength ratios given by the equation of Pillai and Parthasarathy (1977) are close to the experimental axial strength ratios. It may also be noted that, in general, the values of axial strength ratios decrease non-linearly for the increase of SR. However the rate of decrease of axial strength ratios for SR up to 21 is gradual, and rapid in the case of SR ranging from 21 to 30. It may be due to the onset of buckling characteristics of SCC wall panels, which takes place at SR of about 21 and as the SR increases beyond 21 the buckling action gets accelerated and faster leading to lower values of axial strength ratios. The experimental values of axial strength ratios of SCC wall panels were higher than NC wall panels considered in this study. The above observations reveal that a separate model is to be proposed for predicting the ultimate load of SCC wall panels.

6. Method for predicting the ultimate load of SCC wall panels

The proposed method consists of two steps. The first step involves development of an equation for the ultimate load of SCC wall treating it as a short wall. Subsequently this equation is modified to account for the effect of SR and AR on the ultimate load of walls. The following assumptions are made while formulating the equation for predicting the ultimate load of SCC wall panels.

- (i) The load on the panel is reasonably concentric: i.e., $e/t \leq 1/6$
- (ii) The panel contains at least nominal amounts of steel in vertical and horizontal directions as specified in ACI 318-08
- (iii) Considering the same trend and extrapolating the points of experimental axial strength ratios, the SR will be limited to a maximum value of 43 at which the axial strength ratio becomes zero (Fig. 17) and
- (iv) AR is limited to a maximum value of 2.

The largest eccentricity at which a load can be applied to a wall, without cracking of the wall is $t/6$. This load case can be approximated by a rectangular stress block extending from the compressed face of the wall for a distance of two-thirds of thickness of the wall (MacGregor and Wight 2005). The force per horizontal length of wall, L is

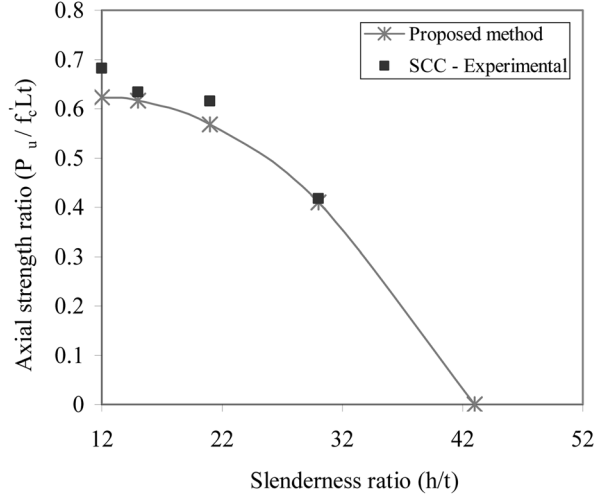


Fig. 17 Comparison of proposed method (Eq. (10)) with experimental values

$$P_{us} = 0.85 f'_c (2/3) Lt \quad (1)$$

$$P_{us} = 0.566 f'_c Lt \quad (2)$$

This was rounded off to $0.56 f'_c Lt$ and the Eq. (2) is rewritten as

$$P_{us} = 0.56 f'_c Lt \quad (3)$$

According to ACI 318 (2008), the ultimate load of RC wall is determined based on the assumption that the minimum ratio of area of reinforcement to the gross area of concrete shall be 0.0015 and 0.0025 in the vertical and horizontal directions respectively. However in the case of thin wall panels these ratios may be higher and hence the effect of reinforcement has to be included appropriately in the model for predicting the ultimate load (Zielinski *et al.* 1982). Thus the Eq. (3) is modified as follows.

$$P_{us} = 0.56 [f'_c Lt + (f_y - f'_c)Asc] \quad (4)$$

Where, P_{us} – Theoretical ultimate load of a short wall

$[(f_y - f'_c)Asc]$ – accounts for the effect of reinforcement

In order to introduce the effect of SR on the ultimate load of walls, the values of (P_{ue}/P_{us}) are plotted against the (h/t) as shown in Fig. 13. The best fit equation obtained for this plot is

$$(P_{ue}/P_{us}) = 0.9271 + 0.0259 (h/t) - 0.0011(h/t)^2 \quad (5)$$

The above equation is rewritten in terms of (h/kt) as given by the ACI 318 (2008) and other researchers (Oberlender and Everard 1977, Saheb and Desayi 1989). Thus, the equation for (P_{ue}/P_{us}) is written as

$$(P_{ue}/P_{us}) = \left[1 + \left(\frac{h}{36t} \right) - \left(\frac{h}{29t} \right)^2 \right] / 1.0786 \quad (6)$$

Where, P_{ue} – experimental ultimate load

Similarly the effect of AR on the ultimate load of walls was obtained by plotting the values of (P_{ue}/P_{us}) against the values of (h/L) as shown in Fig. 14. The best fit equation obtained from the figure is

$$(P_{ue}/P_{us}) = 1.1451 - 0.1245(h/L) \quad (7)$$

The effect of AR can be obtained in terms of (h/kL) , similar to the procedure adopted by Saheb and Desayi (1989), and the equation is rearranged as

$$(P_{ue}/P_{us}) = [1 - (h/9L)]/0.8733 \quad (8)$$

Combining Eq. (4), Eq. (6) and Eq. (8), an equation is proposed for predicting the ultimate load of SCC wall panels and the equation is

$$P_{ue} = 0.57 [f'_c Lt + (f_y - f'_c) Asc] \left[1 + \left(\frac{h}{36t} \right) - \left(\frac{h}{29t} \right)^2 \right] \left[1 - \left(\frac{h}{9L} \right) \right] \quad (9)$$

As the value of experimental ultimate load P_{ue} must be equal to the predicted ultimate load P_u , the term P_{ue} in Eq. (9) is replaced by P_u and is given as

$$P_u = 0.57 [f'_c Lt + (f_y - f'_c) Asc] \left[1 + \left(\frac{h}{36t} \right) - \left(\frac{h}{29t} \right)^2 \right] \left[1 - \left(\frac{h}{9L} \right) \right] \quad (10)$$

Where, P_u - predicted ultimate load

f'_c - cylinder compressive strength of concrete

L - length of the wall panel

t - thickness of the wall panel

f_y - yield strength of steel

Asc - area of compression reinforcement

h - height of the wall panel

In the above equation the first term on the right hand side indicates the ultimate load of wall panel treating it as a short wall; the second term indicates the effect of SR and the third term indicates the effect of AR. The values of axial strength ratios were calculated using the proposed method (Eq. (10)) and plotted against slenderness ratio (h/t) as shown in Fig. 17. From the figure it may be noted that the proposed equation predicts the ultimate load of SCC wall panels satisfactorily.

7. Conclusions

1. The development of larger number of finer cracks in SCC wall panels rather than smaller number of wider cracks in NC wall panels indicate a better cracking performance in the case of SCC wall panels. This behaviour will improve the serviceability limit states and durability significantly.

2. SCC wall panels exhibit higher ductility than the NC wall panels. Hence SCC wall panels appear to be ideal structural elements in the case of seismic resistant structures.

3. The methods available in the literature for the design of RC walls did not compare satisfactorily with test results of SCC wall panels and found to be highly conservative. Hence a method is

proposed to predict the ultimate load of SCC wall panels considering three major parameters such as concrete strength, SR and AR. The computed values of ultimate load by the proposed method compare satisfactorily with the experimental values.

References

- ACI Committee 318 (2008), "Building code requirements for structural concrete (ACI 318-08) and commentary (318R-08)", *American Concrete Institute*, Farmington Hills, MI, USA.
- AS3600-1994 (1994), "Concrete structures", *Standards Association of Australia*, North Sydney, NSW, Australia.
- Benayoune, A., Samad, A.A.A., Abang Ali, A.A. and Trikha, D.N. (2007), "Response of pre-cast reinforced composite sandwich panels to axial loading", *J. Constr. Buil. Mater.*, **21**, 677-685.
- Doh, J.H. (2002), "Experimental and theoretical studies of normal and high strength concrete wall panels", PhD thesis, Griffith University, Gold Coast Campus, Australia.
- Domone, P.L. (2006), "Self-compacting concrete: An analysis of 11 years of case studies", *Cement Concrete Comp.*, **28**, 197-208.
- EFNARC (2002), "Specifications and guidelines for self compacting concrete", *European Federation of National Trade Associations*, Surrey, UK.
- Fragomeni, S. (1995), "Design of normal and high strength reinforced concrete walls", PhD thesis, University of Melbourne, Melbourne, Australia.
- Ganesan, N., Indira, P.V. and Rajendra Prasad, S. (2009), "Ultimate strength of reinforced concrete wall panels", *Int. J. Earth Sci. Eng.*, **2**(4), 340-350.
- IS 1489 (Part 1) (1991), "Indian standard code of practice for Portland-Pozzolana Cement-Specification, (Fly Ash based)", *Bureau of Indian Standards*, New Delhi.
- IS 383 (1970), "Indian standard code of practice for specification for coarse and fine aggregate from natural sources for concrete", *Bureau of Indian Standards*, New Delhi.
- IS 10262 (1982), "Indian standard code of practice for recommended guidelines for concrete mix design", *Bureau of Indian Standards*, New Delhi.
- Kripanarayanan, K.M. (1977), "Interesting aspects of the empirical wall design equation", *J. Proc.*, **74**(5), 204-207.
- Luciano, G. and Andrea, V. (2008), "Strength and ductility of HSC and SCC slender columns subjected to short-term eccentric load", *ACI Struct. J.*, **105**(3), 259-269.
- MacGregor, J.G. and Wight, J.K. (2005), *Reinforced Concrete – Mechanics And Design*, (4 Edition), Pearson Prentice Hall Edition.
- Oberlender, G.D. and Everard, N.J. (1977), "Investigation of reinforced concrete wall panels", *J. Proc.*, **74**(6), 256-263.
- Pillai, S.U. and Parthasarathy, C.V. (1977), "Ultimate strength and design of concrete walls", *Buil. Environ. J.*, **12**, 25-29.
- Precast/Prestressed Concrete Institute (2003), "Interim guidelines for the use of self-consolidating concrete in precast/prestressed concrete institute member plants", *TR-6-03*, Chicago, IL.
- Saheb, S.M. and Desayi, P. (1989) "Ultimate strength of RC wall panels in one-way in-plane action", *J. Struct. Eng-ASCE*, **115**(10), 2617-2630.
- Zielinski, Z.A., Troitsky, M.S. and Christodulu, H. (1982), "Full-scale bearing strength investigation of thin wall-ribbed reinforced concrete panels", *ACI J.*, **79**(4), 313-321.